Giant Magnetoresistance (GMR) Magnetometers

Candid Reig and María-Dolores Cubells-Beltrán

Abstract Since its discovering in 1988, the Giant Magnetoresistance (GMR) effect has been widely studied both from the theoretical and the applications points of view. Its rapid development was initially promoted by their extensive use in the read heads of the massive data magnetic storage systems, in the digital world. Since then, novel proposals as basic solid state magnetic sensors have been continuously appearing. Due to their high sensitivity, small size and compatibility with standard CMOS technologies, they have become the preferred choice in scenarios traditionally occupied by Hall sensors. In this chapter, we analyze the main properties of GMR sensors regarding their use as magnetometers. We will deal about the physical basis, the fabrication processes and the parameters constraining their response. We will also mention about some significant application, including developments at the system level.

1 Physical Background

The electric current in a magnetic multilayer consisting of a sequence of thin magnetic layers separated by thin non-magnetic layers is strongly influenced by the relative orientation of the magnetizations of the magnetic layers [1, 2]. More specifically, the resistance of the magnetic multilayer is low when the magnetizations of the magnetics layers are parallel but higher when the magnetizations of the neighbouring magnetic layers are antiparallel. This is due to the spin-dependent scattering. The spontaneous relative orientation between adjacent magnetic layers depend on the the thickness of the spacer layer. Then, by applying an external magnetic field, a change from antiferromagnetic to ferromagnetic (or viceversa) coupling can be achieved, so changing the resultant resistance value.

C. Reig (✉) · M.-D. Cubells-Beltrán
University of Valencia, Valencia, Spain
e-mail: candid.reig@uv.es

M.-D. Cubells-Beltrán
e-mail: m.dolores.cubells@uv.es

© Springer International Publishing Switzerland 2017

A. Grosz et al. (eds.), *High Sensitivity Magnetometers*, Smart Sensors, Measurement and Instrumentation 19, DOI 10.1007/978-3-319-34070-8_8

The magnetoresistance (MR) ratio is, then, generally defined as:

$$\frac{\Delta R}{R} = \frac{R^{\uparrow\downarrow} - R^{\uparrow\uparrow}}{R^{\uparrow\uparrow}} \tag{1}$$

Such behaviour has important applications, initially focusing on magnetic information storage technology. In this sense, P. Grunberg and A. Fert received the Nobel Prize in Physics in 2007 for the discovering of the effect [3].

There are several kind of structures that can display GMR effect [4, 5]. In fact, there have been described and used granular materials with such effect [6]. For engineered applications, multilayer structures are preferred due to their integration feasibility [7]. Typical multilayered structures consist of two or more magnetic layers of a Fe–Co–Ni alloy, as can be permalloy, separated by a very thin non magnetic conductive layer, as can be Cu [5], as sketched in Fig. 1 (left). With magnetic films of about 4–6 nm width and a conductor layer of about 35 nm, magnetic coupling between layers is slightly small. With this configurations, MR levels of about 4–9 % are achieved, and spreading the linear ranges of about 50 Oe [5], good for sensing applications. The figures of merit of these devices can be improved by continuously repeating the basic structure.

Spin valves are a particular configuration of a sandwich structure. In spin valves, an additional antiferromagnetic (*pinning*) layer is added to the *top* or *bottom* part of the structure, as shown in Fig. 1 (right). In this sort of structures, there is no need of an external excitation to get the antiparallel alignment. In spite of this, the pinned direction (easy axis) is usually fixed by raising the temperature above the knee temperature (at which the antiferromagnetic coupling disappears) and then cooling it within a fixing magnetic field. Obviously, so obtained devices have a temperature limitation below the knee temperature. Typical values displayed by spin valves are a MR of 4–20 % with saturation fields of 0.8–6 kA/m [4].

For linear applications, and without excitation, pinned (easy axis) and free layers are preferably arranged in a crossed axis configuration (at 90°), as depicted in Fig. 2. In this way, the linear range is improved and the sign of the external field is detected without the need of an additional magnetic biasing. The response this structure is given by Freitas et al. [8]:

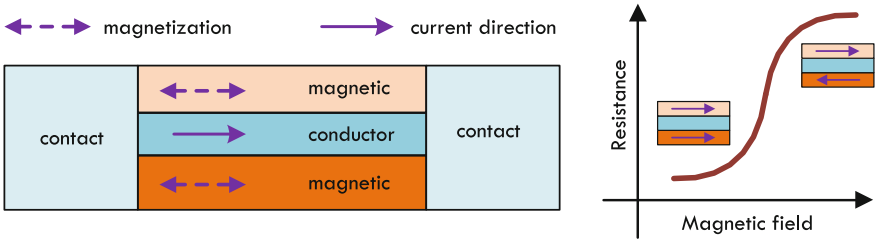

Fig. 1 (*left*) Basic GMR multilayer structure, (*right*) typical response of a basic GMR structure

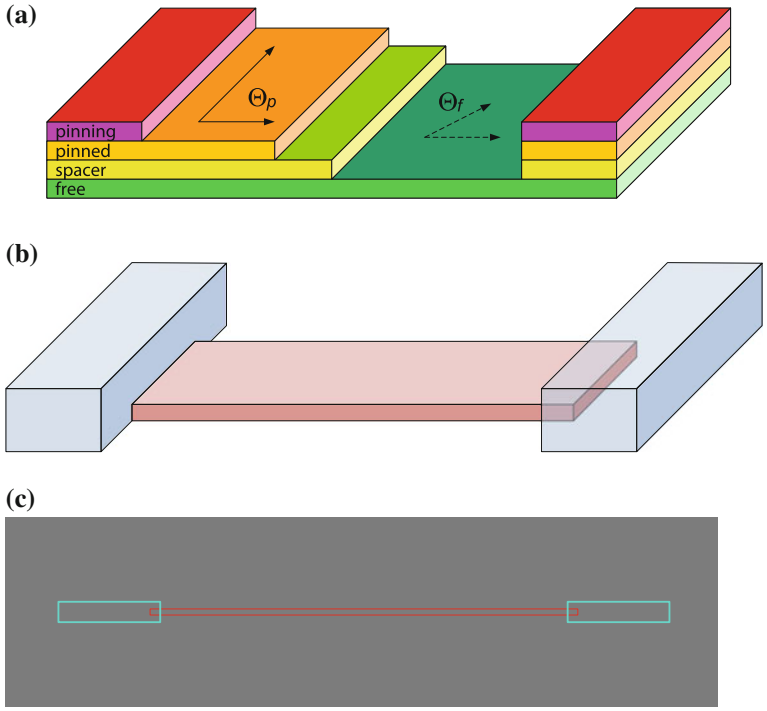

Fig. 2 Basic spin valve scheme: **a** multilayer structure in crossed axis configuration, **b** typical implementation, **c** simplest lithography masks set

$$\Delta R = \frac{1}{2}\left(\frac{\Delta R}{R}\right) R_{\square} \frac{iW}{h} \cos\left(\Theta_p - \Theta_f\right) \tag{2}$$

where $(\Delta R/R)$ is the maximum MR level (5–20 %), $R_{\square}$ is the sensor sheet resistance 15–20 $\Omega/\square$), L is the length of the element, W is its width, h is the thickness, i is the sensor current, and Θ_p and Θ_f are the angle of the magnetization angle of pinned and free layers, respectively. Assuming uniform magnetization for the free and pinned layers, for a linearized output, $\Theta_p = \pi/2$ and $\Theta_f = 0$.

As a practical example, in [9], the spin valve structure was deposited by ion beam sputtering (IBD) onto 3″ Si/SiO_2 1500 Å substrates with a base pressure of $1.0 \times 10^{-8} - 5.0 \times 10^{-8}$ Torr. For IBD deposition, a Xe flow was used for a deposition pressure of 4.1×10^{-5} Torr. The spin valve structure was Ta(20 Å)/NiFe(30 Å)/CoFe(20 Å)/Cu(22 Å)/CoFe(25 Å)/MnIr(60 Å)/Ta(40 Å). This structure has demonstrated to give magnetoresistance responses of about 6–7 %, linear ranges of about 20 Oe and sheet resistivities of about 10–15 $\Omega/\square$) [9]. Deposition rates ranged from 0.3 to 0.6 Å/s. A 40 Oe field was applied to the substrates during the deposition step in order to state the easy axis in the pinned and free layers. The

wafer was 90° rotated between both depositions to ensure a crossed-axis spin valve configuration.

Nano-oxide layers (NOL) inserted in the pinned layer and above the free layer have been found to increase the magnetoresistance ratio up to 19 % [10]. The enhancement of GMR is attributed to the specular scattering effect of the conduction electrons at the metal/insulator interfaces.

In [11], the specular spin valve structure was Ta(3 nm)/NiFe(3 nm)/MnIr(6 nm)/CoFe(1.6 nm)//NOL//CoFe(2.5 nm)/Cu(2.5 nm)/CoFe(1.5 nm)/NiFe(2.5 nm)//NOL//CoFe(2.0 nm)/Ta(0.5 nm). NOL layers were formed in a 15 min natural oxidation step at atmospheric pressure in the deposition tool load lock. The natural oxidation process, keeping its simplicity, has proven to be well effective. Finally, the samples were annealed at 270 °C under vacuum and cooled under a 3 kOe magnetic field applied parallel to the pinned and free layer easy axis.

Giant magnetoresistance can also find in other structures. We collect two illustrative examples. Pena et al. [12] report on giant magnetoresistance in ferromagnet/superconductor superlattices. On the other hand, Pullini et al. [13] describe GMR in multilayered nanowires. In any case, a magnetic/non-magnetic interface is required in order to allow the spin-electron scattering producing the effect.

2 Fabrication

The fabrication of giant magnetoresistance (GMR) devices involves a sort of techniques including deposition, patterning and encapsulation in a similar fashion to those related to standard CMOS processes. Because doping and implantation are not required, they can be considered as low temperature processes. As a guideline, three to five lithography steps are required for fabricating basic GMR devices. They can be deposited on silicon wafers but glass, sapphire or flexible substrates can also be considered.

On Bi-CMOS processes, silicon, silicon oxide and aluminum are the basis materials, as well as the dopants (Boron, Phosphorus, Arsenic, Antimony and related compounds). In the case of GMR devices, the fabrication of magnetic layers requires the use of additional magnetic materials (Iron, Cobalt, Nickel, Manganese, and their alloys), different metals (e.g. Copper, Ruthenium) and additional oxides (Al_2O_3, MgO …), not usually found in conventional semiconductor facilities. Each of these materials has particular requirements in terms of deposition technology and conditions or system contamination that need to be specifically considered and optimized. As a high-lighting example we should mention the deposition of layers with preferentially aligned magnetic moment which requires the use of a polarizing magnet placed inside the deposition system, therefore not easily compatible with hot deposition tools.

2.1 Deposition

As before mentioned, GMR structures are composed of multilayered engineered structures based on nanometric to sub-nanometric thick layers of ferromagnetic materials (e.g.: Co, CoFe, NiFe) separated by a non-magnetic spacer (Cu). Isolation layers are also commonly required. Therefore, adequate deposition techniques namely those using ultra-high vacuum systems and providing a thorough control of the thickness of the deposited layers are essential for the proper functionality of so obtained devices.

2.1.1 Sputtering

Cathodic sputtering is one of the more common physical vapor deposition technique used for depositing thin films onto substrates. Such sputtering process occurs when an accelerated ion hits a solid target material. If the ion kinetic energy is high enough, atoms are extracted from the matrix. A vacuum reaction chamber (usually lower than 10^{-7} Torr) is required. A high voltage is applied to the target holder so producing an electrical discharge that allows the ionization of the gas and hence leads to the plasma. The produced ions are then attracted toward the cathode, hitting the target. The ions with energy above the threshold can extract atoms from the target material. These atoms are deposited onto the substrate, usually facing the target, and thus forming a layer of material.

Regarding specific GMR devices, this method offers the possibility to deposit from a target composed of different materials (alloy or mosaic target). Due to this, sputtering is one of the preferred techniques to deposit metallic and magnetic layers in GMR de-vices. It is also commonly used for the deposition of metallic non-magnetic contacts and also insulating oxides.

2.1.2 Ion Beam Deposition (IBD)

The IBD technique is not as extended as traditional sputtering but it provides a good film thickness uniformity and higher deposition control due to the low deposition rates employed, enabling also epitaxial growth under particular conditions and higher deposition textures. Deposition parameters such as ion flux, energy and sputtered species, as well as the angle of incidence, can be more independently controlled. In this case, the plasma is created and confined in an ion gun being then accelerated towards the target through voltage applied into a grid set. Furthermore, the basic configuration of a typical IBD system normally includes an assist gun, used either for assisted deposition or ion-milling etching. An automatically

interchangeable target holder (4–8 targets) can be used in GMR multilayer deposition without vacuum break, with deposition rates below 1 nm/s.

2.1.3 Chemical Vapor Deposition (CVD)

CVD thin films deposition is based on the decomposition and/or reaction of different gaseous compounds. In this way, the considered material is directly deposited onto the substrate surface from a gas phase.

Deposition usually occurs at high temperatures >300 °C, therefore not compatible with magnetic multilayers. However, since the deposition rates can be very large (therefore fast deposition) and it is a conformal deposition (thus, excellent step coverage), this method is mainly used in the deposition of insulating and passivation layers (silicon oxide or silicon nitride) leading to good quality layers with moderate cost equipment.

2.2 Patterning

GMR structures can be patterned in a similar way than common devices in typical CMOS processes. Well-known ultraviolet (UV) lithography through hard or software designed masks, together with physical or chemical etching processes can be used. In this way, a good ratio cost/reliability is achieved with defined features down to ~ 1 μm. The patterning process of a GMR device consists of sequential steps of pattern design and transfer as illustrated in Fig. 3, with typically three lithography steps, including that for opening contacts.

2.2.1 Photolithography

The photolithography process includes three steps: (i) coating of the sample with a proper photoresist (a radiation sensitive polymer solution); (ii) exposure of the resist, patterning a certain design (mask), previously prepared; (iii) development of the transferred pattern.

Coating

The photoresist is deposited onto the surface of the sample by spin-coating, with controlled conditions of speed, time and amount of resist for a proper thickness and homogeneity of the sensitive layer, which is crucial for the lithography resolution [14]. It is usually required a surface pre-treatment (such as hexamethyldisilizane, HMDS) for promoting the adhesion, and a post-treatment (soft-baking, 80–100 °C) for removing solvents and stress.

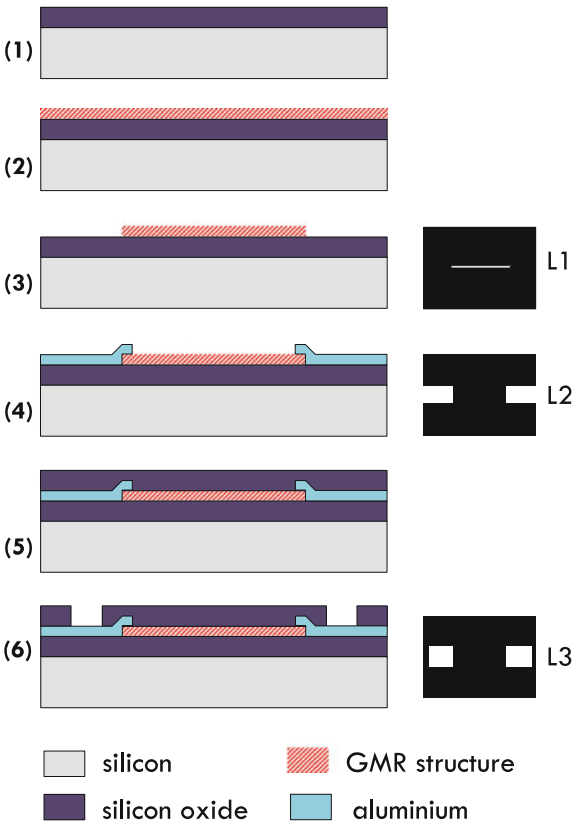

Fig. 3 Typical steps of the patterning procedure in microfabrication of basic GMR devices

Lithography

By using UV radiation (wavelength typically ranging 0.5–0.1 μm) with focused laser beams (direct write systems) or lamps (hard mask aligners), resolutions below 1 μm can be obtained. Due to the commonly limited production volumes of GMR devices, direct write systems are particularly interesting. In this case, a spot of the light beam moves trough the surface in those zones that need to be illuminated, with the help of a precision X-Y system, together with a switching light mechanism. The fabrication of physical masks is, then, not required. This is a versatile and low cost, but slow process (the full exposure of a 150 mm wafer can take more than 12 h, depending on he particular design). If higher resolutions are demanded (<0.5 μm), X-ray, electron or ion beam systems can be used [15].

Development

The development is usually assisted by a soft-baking step before the resist developer is sprayed or spin-coated onto the sample surface. With positive resists, exposed regions have turn soluble during the exposure and are removed at this moment. For negative resits, exposed regions turn harder and remain after

developing. In any case, the sample is then washed to stop the development process and dried. The pattern has been printed into the resist layer.

2.2.2 Pattern transfer techniques

We will consider two options: etching and lift-off.

Etching

It is a process concerning the capability of removal undesired portions of a deposited layer. Such a selective property is provided by the patterned resist mask, but also by the characteristics of the involved layers. The starting point is usually the film to be patterned deposited on a substrate with the desired pattern defined in the top resist mask,

Dry etching. Physical (dry) etching is commonly achieved by using plasma etching (reactive etching or an ion beam system) providing a controlled removal of material. Ion beam etching (ion milling), in particular, offers slow (below 0.2 nm/s) but very controlled and stable etching ratios and it is usually used for the patterning of GMR devices [15]. It is an anisotropic process with etching efficiency depending on the material type and the incident angle [16].

Wet etching. For chemical (wet) etching, corrosive properties of some substances (usually acids) are used. In this way, wet etching can be patterned with polymer based resists, due to their intrinsic organic nature, resistant to the inorganic acids action. Tables with specific etchers for the different materials, with associated speeds can be found in the literature [17]. Due to its aggressive and isotropic nature, wet etching is not commonly used for patterning GMR structures and is mostly used for processes like opening contacts/vias.

3 Noise

Real performances of GMR magnetometers can only be estimated when compared with their intrinsic noise sources. The noise power spectrum density (PSD) is commonly given in V^2/Hz. Often, is much more convenient to use the amplitude spectrum density (ASD), expressed in $V/\sqrt{Hz}$ for comparison with voltage signals. The sensitivity for a magnetoresistance signal, S_V is usually given in V/V/T. Typical values for GMR sensors are 20–40 V/V/T, e.g., 20–40 nV/nT when they are biased with 1 V. For comparing different sensors, it is recompensable to use the field equivalent noise power spectra density, sometimes called *detectivity*. It corresponds to the PSD divided by the sensitivity. For example, if a sensor displays a noise of $10\,nV/\sqrt{Hz}$ at a given frequency and a sensitivity of 25 V/V/T, its detectivity will be 400 pT for 1 V bias.

3.1 Types of Noise in GMR Magnetometers

3.1.1 Thermal Noise

The most relevant noise is the thermal noise (also called Johnson-Nyquist noise or white noise), which is directly related to the resistance of the sensor. It is a *white* noise, so it is independent of the frequency. It was first observed by Johnson [18] and interpreted by Nyquist [19]. It is expressed as:

$$S_V(\omega) = \sqrt{4Rk_BT} \tag{3}$$

where R is the sensor resistance, k_B is the Boltzmann constant and T is the temperature. For example, a 1 kΩ resistor at room temperature has $4\,\mathrm{nV}/\sqrt{\mathrm{Hz}}$.

3.1.2 1/*f* Noise

The origin of the 1/*f* noise or 'pink' noise or Flicker noise is on resistance fluctuations, so it can only revealed by applying a current into the sensor. Its dependence with the frequency is described by the following phenomenological formula:

$$S_V(\omega) = \frac{\gamma_H R^2 I^2}{N_C f^\beta} \tag{4}$$

where γ_H is a dimensionless constant proposed by Hooge [20], R is the sensor resistance, I is the bias current, N_C is the number of current carriers, f is the frequency and β is an exponent typically in the order of 1. 1/*f* noise can exhibit a non magnetic and a magnetic component with possible different slopes. The size and the shape of the sensors have a strong effect on the 1/*f* noise. Due to its average nature, and as followed by Ec. 4, small GMR sensors display more 1/*f* noise than bigger ones. By considering equally thin sensors, the 1/*f* noise is roughly inversely proportional to their area [21].

3.2 Noise Measurement in GMR Devices

Noise measurement is a difficult task that needs to be carefully performed. A standard measurement system should comprise the sensor (device-under-test, DUT), a low noise biasing source (usually batteries), a low noise amplifier (it can be composed of different stages), filtering and acquisition/processing system, as this depicted in Fig. 4. In some occasions, last two parts can be replaced by a spectrum analyzer. A particular implementation is also shown in Fig. 4 including a National Instruments data acquisition (DAQ) card (24 bits of resolution, 200 kHz bandwidth

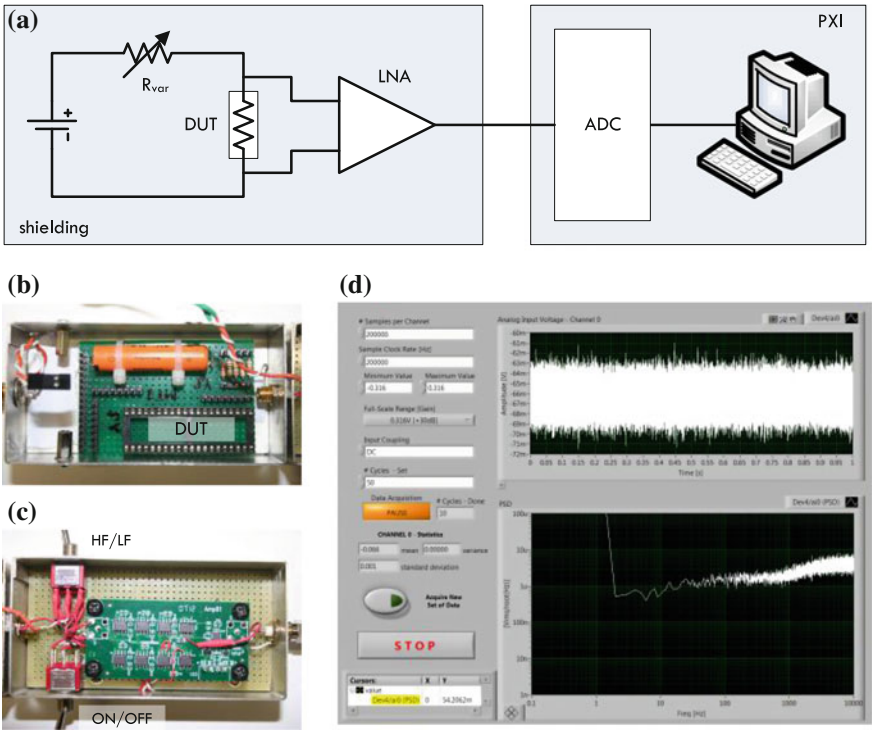

Fig. 4 Noise measurement system: **a** basic setup, **b** detail of the bias and shielding of the DUT, **c** a specifically designed LNA, **d** aquisition and processing software

and noise spectral density of $8\,\mathrm{nV}/\sqrt{\mathrm{Hz}}$ at 1 kHz) and a low-noise amplifier (2 nV/$\sqrt{\mathrm{Hz}}$ noise in a frequency band from 0.3 Hz to 100 kHz and voltage gain of 1000). Devices and bias batteries are shielded. A LabView program is used for controlling the system and obtaining the ASD.

As a representative example, we will give noise data on spin valves based on multilayered structures [Ta(20 Å)/NiFe(30 Å)/CoFe(20 Å)/Cu(22 Å)/CoFe(25 Å)/MnIr(60 Å)/Ta(40 Å)] patterned on strips of $3 \times 200\,\mu\mathrm{m}^2$. Measured sensitivity was 20 mV/mT (1 mA bias). Measured bandwidth was above 1 MHz [22]. The measured noise is shown in Fig. 5a, b. The $1/f$ behaviour is clearly observed and the thermal noise limit well defined. If we take into account the measured sensitivity, we can draw the detectivity understood as the field equivalent noise, that is drawn in Fig. 5c, d. The benefits of the frequency is clearly stated. The increase of the bias current has an impact on the field detectivity at higher frequencies, but there is no effect in the $1/f$ regime [21].

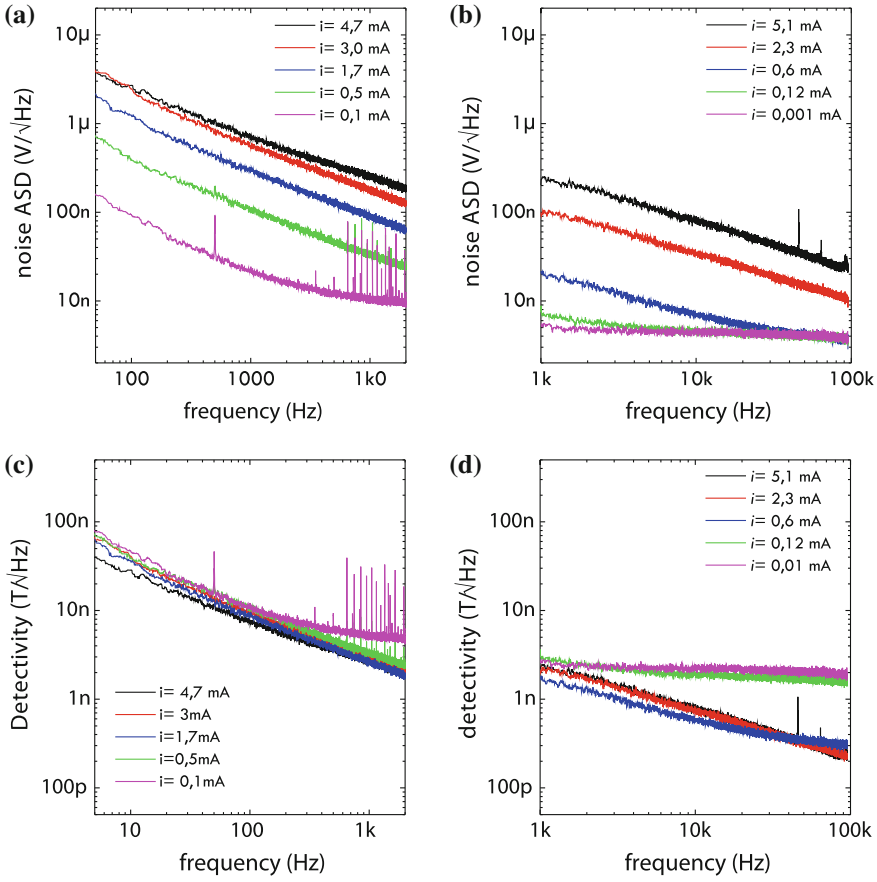

Fig. 5 Noise measurement data on $3 \times 200\ \mu m^2$ spin valves as described in [22]: **a** low frequency noise, **b** high frequency noise, **c** low frequency detectivity, **d** high frequency detectivity

3.3 Improving the Detectivity

Once the main parameters have been introduced, we follow with some suggestion for improving the detectivity in GMR based magnetometers, as discussed in [23].

- Structures with high sensitivity (high MR level) should be considered in order to maximize the output signal. Then, the signal to noise ratio (SNR) needs to be calculated. In this sense, tunnel magnetic resistance (TMR) devices display sensitivities higher than those from GMR, but with a noise level that is typically three times higher. Then, a triple MR level is required for achieving the same SNR. On the other hand, linear ranges should be kept as narrow as possible in

Table 1 Field equivalent noise of GMR as dependant on the dimensions

	Size	Noise at 1 Hz	White noise	Power consumption
Small GMR	150 × 4 μm^2	10 nT	50 pT	5 mW
Large GMR	1 mm^2	100 pT	20 pT	100 mW

order that the pendent in the response (and then the sensitivity) is as high as possible [see Fig. 1 (right)]

- Due to the statistical nature of noise, this is reduced with the increasing of the sensor size, by means of the Hooge parameter. From [21], the values in Table 1 can be extracted.
- The frequency of operation should be stated as high as possible in order to minimize the 1/*f* noise effect. This can hardly done by modulating the measured field with additional loops or by placing the sensing elements onto oscillating cantilevers [23].
- The use of flux guide concentrators allows, in some cases, to have a magnetic field amplification up to one hundred. In addition, the deposition of high permeability materials is compatible with the patterning and deposition processes described above.

4 Thermal Effects

The temperature is always a limiting parameter in electronics. Every electronic device has temperature depending response arising from its physical nature. Regarding specific GMR electrical current sensors, not only the resistance (and then the sensor impedance) varies with the temperature. Also the MR level (and then the sensitivity) does.

The resistance of GMR sensors, like common resistances, is a function of the temperature. For GMR based devices, and in the usual range of utilization, this dependence can be considered as linear, and can be defined by a temperature coefficient (TEMPCO) as following:

$$TCR(\%) = 100 \times \frac{1}{R_{T_0}} \frac{\Delta R}{\Delta T} \tag{5}$$

An analogue relationship can be defined for the thermal dependence of sensitivity, as:

$$TCS(\%) = 100 \times \frac{1}{S_{T_0}} \frac{\Delta S}{\Delta T} \tag{6}$$

When a full bridge configuration is considered, this thermal dependence is partially compensated and is expected to be low. Due to the inherent voltage offset of sensors configured as bridges, the temperature drift of the offset voltage must be specified::

$$TCV_{off}(\%) = 100 \times \frac{\frac{\Delta V_{off}}{\Delta T}}{V_{off,T_0}} \tag{7}$$

Moreover, the output voltage has also a thermal dependence, defined as:

$$\begin{aligned} TCV_o(\%) &= 100 \times \frac{1}{\Delta T}\frac{V_{o,T_i} - V_{o,T_0}}{V_{o,T_0}} \\ V_{o,T_i} &= V_{out,T_i} - V_{off,T_i} \end{aligned} \tag{8}$$

Experimental parameters are only related to the nature of the GMR structures, and they have been measured elsewhere. In Fig. 6 we show typical values for full bridge sensors composed of equal spin valve elements, as described in [22]. From these graphs we can extract $TCR \approx 0.11$ %/°C, $TCV_{off} < 10$ μV/°C and $TCS \approx -0.15$ %/°C.

Compensation techniques

Assumed that thermal effects cannot be completely eliminated, various methods of temperature compensation have been reported in the literature addressed to reduce the thermal drift output of Wheatstone bridge type sensors. These methods can be differentiated as noninvasive and invasive. As noninvasive we mean a technique consisting of the addition of different circuit elements in series or parallel to the bridge in order to reduce its thermal drift, as described, for example in [24]. A temperature sensor, a fixed resistor, some kind of active network (diode or transistor) or a fixed current source have been successfully applied. This way, the addition of one of the above elements results in a change of the bridge supply voltage due to the temperature variation, which produces a valid compensation.

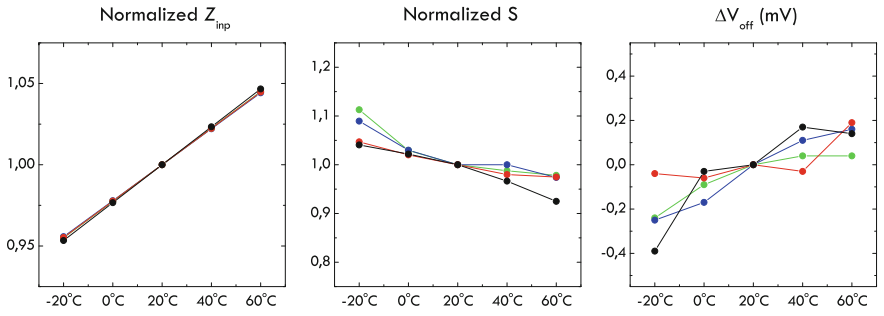

Fig. 6 Experimental thermal parameters of typical GMR structures

A slightly different approach consists of the connection of a temperature variable gain instrumentation amplifier in cascade at the output of the bridge. On the other hand, a Wheatstone bridge can also be temperature compensated by means of the modification of its original configuration. In this case, we should ensure that the terminals of the bridge are externally accessible. This group of techniques can be considered as invasive, due that the conditioning circuitry in common commercial sensors make the bridge terminals often inaccessible. An excellent revision of these works is made in [25]. In addition, in the same work is presented a novel application of the Generalized Impedance Converter (GIC) as a thermal compensating biasing circuit for specific magnetoresistive sensors.

5 Electronic Interfaces

From the macroscopic point of view, a GMR sensor behaves as a resistance. In this sense, in order to get a useful electrical signal, traditional schemes applied to resistive sensors can be considered.

5.1 Resistive Bridges

Although single elements or basic voltage dividers can be also considered, to arrange a resistive senor in a bridge configuration has clear advantages in terms of the signal level, linearization, voltage offset and immunity against external undesired perturbations. As a clear example, we can observe the benefits of such configuration from data in 6. In this sense, we can make use of bridges with a unique sensing element, half bridges or full Wheatstone bridges. For getting half bridge sensors, and due to the requirement of polarization of the magnetic moments of the layers, two of the four sensing elements must be inactive, usually got by depositing patterned magnetic shielding layers [26]. It should be noted that, if a full Wheatstone bridge is considered, the fabrication involves two steps (see Fig. 7).

5.2 Amplification

Due to the low signals involved, low noise amplifiers (LNA) are usually necessary. Noise sources in operational amplifiers can be:

- *Input-referred voltage noise*. It can be modeled with a noise voltage source. As an example, such a noise is typically : $30\,\mathrm{nV}/\sqrt{\mathrm{Hz}}$ @1 kHz in a 741 general purpose opamp and lower than $1\,\mathrm{nV}/\sqrt{\mathrm{Hz}}$ in an specific LNA.

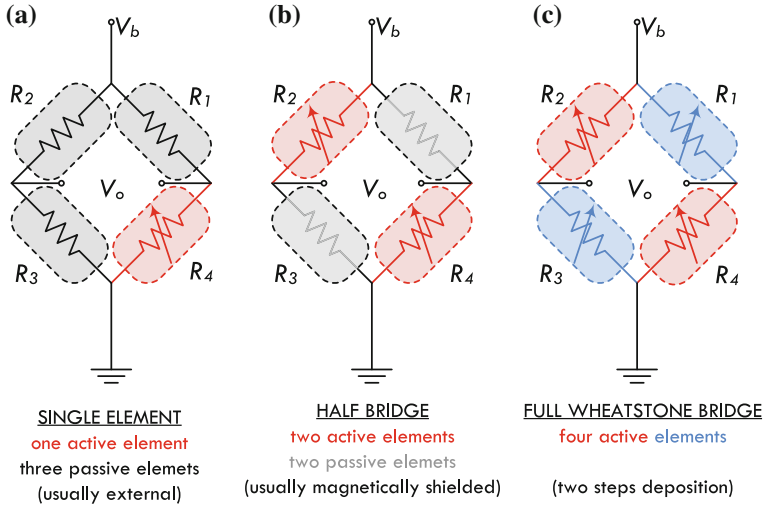

Fig. 7 Arrangements of GMR elements in bridges: **a** Single element, **b** Half bridge, **c** Full wheatstone bridge

- *Input-referred current noise*. It can be modeled as two noise current sources pumping currents through the two differential input terminals). Its value can range from : $10\,\text{pA}/\sqrt{\text{Hz}}$ @1 kHz in general purpose amplifiers to : $10\,\text{fA}/\sqrt{\text{Hz}}$ @1 kHz in specific LNAs.
- *Flicker* (1/*f*) *noise*. Due to the fabrication process, the IC device layout and the device type. It has a rate of $\sim$3 dB/oct for CMOS amplifiers, $\sim$4.0 dB/oct for bipolar amplifiers and $\sim$5 dB/oct for JFET amplifiers,

In this sense, lock-in amplifiers (LIA) [27] and *chopper* amplifiers [28] are the preferred choices.

5.3 Biasing

The correct use of GMR devices implies a proper biasing scheme both from the electric and magnetic point of view. Assuming a resistor bridge configuration, a constant voltage source can be used to feed the sensor, through two opposite vertex of the bridge. The differential output voltage is taken from the remaining pins. Nevertheless, it has been demonstrated that thermal characteristics (temperature drifts) of spin valve based sensors are notably improved by using a constant current source for the sensor feeding [29]. In addition, it has been demonstrated that an ac biasing applied GMR based devices notably improves their performance in terms of linearity, hysteresis, offset and noise [30].

Once the sensor is fed and the bias point set, it can be slightly modified by applying an external magnetic field. This external magnetic field adds (with sign) to

the measured signal and the operation point is then shifted. In a certain way, an offset correcting coil can also be understood as an additional biasing, as presented here. When no helping coils are present, a permanent magnet can also be used. In this case the system has to be carefully designed. A proper magnetic biasing can, for example, to convert to bipolar a GMR device, by displacing the quiescent point to the middle of the output function [30].

5.4 Resistance to Time Approaches

Regarding interfacing, in typical resistor-based sensor applications (such as GMR), the resistive sensing devices are usually dc biased. The generated output signal is taken as an analogue dc voltage level, by employing traditional resistance-to-voltage (*R–V*) conversion approaches and, commonly, by also making use of amplifiers and filters, as previously described. As well known, these voltamperometric solutions usually display undesired voltage offsets that need to be specifically calibrated/corrected or taken into account. When compared with *R–V* converters, front-end schemes using ac excitation have been demonstrated highly advantageous for wide range devices or with unknown nominal/baseline values by improving the immunity to voltage offset, noise and frequency disturbs [15]. These approaches perform resistance-to-frequency (*R–f*) or voltage-to-frequency (*V–f*) conversions so providing a direct quasi-digital output whose frequency depends on the sensor resistance value. In addition, since the ac excitation of the sensor is made through a closed feedback loop, the output frequency is theoretically independent from the power supply level. They generally do not require any calibration procedure and/or manual adjustments and the output signal can be directly connected to the digital part of a system, making these solutions particularly interesting for A/D mixed-signal applications. Moreover, these solutions can be easily used in integrated CMOS designs and SoCs since they are typically implemented with a reduced number of active/passive components.

We can consider several approaches as described in Fig. 8.

A simple astable multivibrator implemented with transistors (not necessarily bipolar), as this depicted in Fig. 8a has an oscillation period given by:

$$T = \ln(2)(R_2C_1 + R_3C_2) \tag{9}$$

then, by making R_2 and/or R_3 variable, we get our objective.

An oscillator can also be implemented by using an integrated 555 circuit, as shown in Fig. 8b. In this case, we get a square wave with a high level during t_1 and a low level during t_2, being:

$$t_1 = \ln(2)(R_1 + R_2)C; t_2 = \ln(2)(R_2)C \quad \text{so} \quad T = \ln(2)(R_1 + 2R_2)C \tag{10}$$

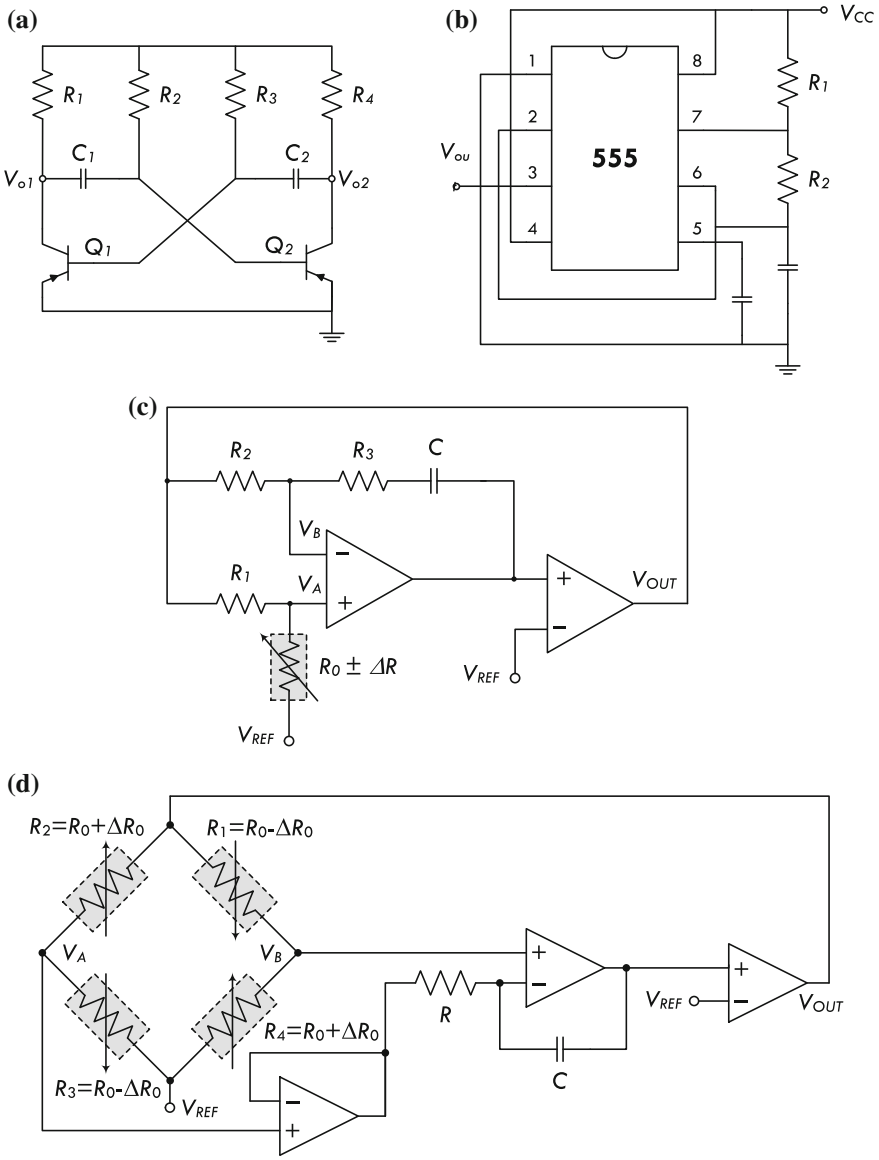

Fig. 8 Differente *R*-to-*t* approaches for resistive GMR devices: **a** basic transistor based astable, **b** astable with 555 IC, **c** circuit with operational amplifiers for single resistors, **d** circuit with operational amplifiers for resistive bridges

More complex approaches can be developed with active elements like opamps as displayed in Fig. 8c and detailed in [31]. In this case,

$$T = \frac{4C_1}{R_1} R_0 (R_0 \pm \Delta R_0) - R_1 R_3 \tag{11}$$

If we are dealing with resistive bridges, we can make use of the circuit in Fig. 8d, where:

$$f = \frac{1}{2RC} \left(\frac{R_4}{R_1 + R_4} \frac{R_3}{R_2 + R_3} \right) \tag{12}$$

Circuits shown in Fig. 8c, d have been successfully used with discrete elements and in integrated circuit form and for GMR spin valve sensing elements and bridges for sub-mA electric current measurements, as described in [31]. Obtained oscillograms are shown in Fig. 9. As observed, sensitivities of 0.8 Hz/mA and 0.68 Hz/μA are obtained which are excellent numbers for these purposes.

5.5 *Arrays*

Arrays of sensors are required for specific applications such as non-destructive evaluation/testing (NDE/NDT) [32, 33], bio-technology systems [34–36] or other magnetic imaging requirements [37, 38]. In general, the access to each individual element involves two electrical/physical connections resulting in a total of $2 \times [N \times M]$ connections. In these particular conditions, read out interfaces for such arrays are a matter of concern [39, 40], usually involving analogue multiplexers and shared amplifiers [41].

5.6 *Compatibility with CMOS Technology*

Non Volatile Electronics (NVE) was the first company in merging both technologies by using a dedicated 1.5 m BiCMOS technology [42]. Later, Han et al. used chips made by 0.25 m NSC (National Semiconductor Corporation) BiCMOS technology [43], by applying a post-process that employed reactive ion etching for via opening through the passivation, so allowing access to the buried metal layers. Then, by combining the design rules for CMOS chips with the techniques for GMR device microfabrication allows the full integration of these sensors with the required electronics (e.g., bias and conditioning circuits, signal processing, memory elements, etc.). Recent achievements regarding the monolithic integration of GMR structures onto standard CMOS circuitry is summarized in Fig. 10. The fabrication of spin valve based magnetic field sensing devices directly onto processed chips

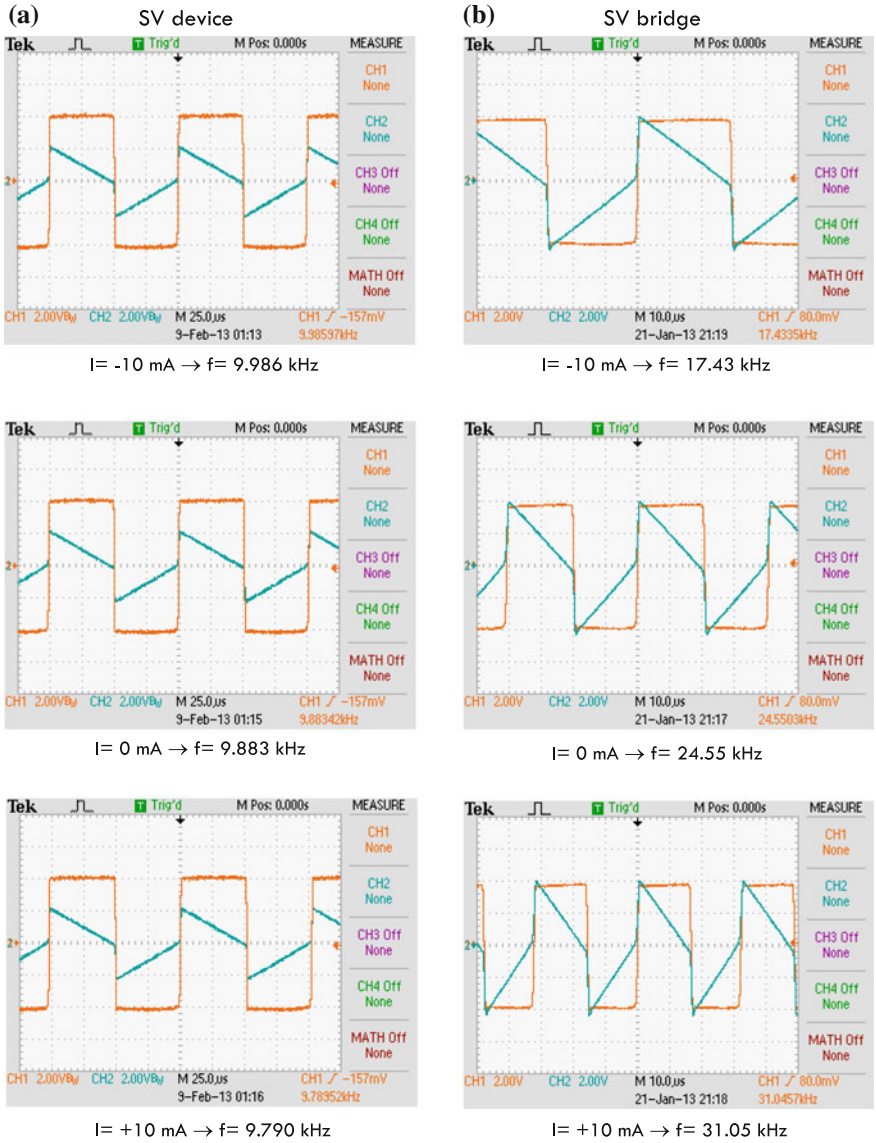

Fig. 9 Experimental oscillograms: **a** from *R*-to-*t* circuit and single GMR devices (Fig. 8c), **b** from *V*-to-*f* circuit and GMR Wheatstone bridges (Fig. 8d)

(from non-dedicated CMOS standard technologies) is described in [44] (see Fig. 10a). Functional devices are successfully developed with an standard 0.35 μm AMS technology and with a non commercial CNM 2.5 μm technology (see Fig. 10b). Due to its extended use, the AMS 0.35 μm process has also recently used for integrated current sensing at the integrated circuit level [45, 46] (see Fig. 10c).

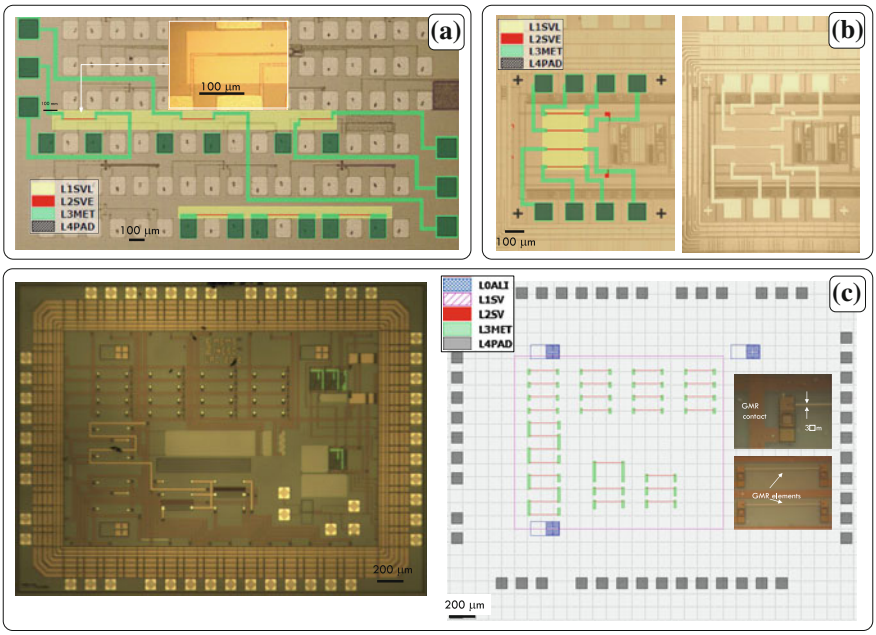

Fig. 10 Real monolithic integration of GMR structures onto pre-processed CMOS chips: **a** wafers from CNM25 non-commercial technology [44], **b** non-dedicated AMS 0.35 µm technology [44], **c** specifically designed AMS 0.35 µm chip for sub-mA current sensing [46]

6 Commercially Available Sensors

GMR is a relatively novel technology. At this moment, up to our knowledge, only few companies (NVE, Infineon and Sensitec) have released GMR linear sensors to the market, beyond the preliminary application on read heads. Other companies include anisotropic magnetoresistance (AMR) based sensors to their portfolio (Honeywell, Zetex, Sypris, Philips and ADI).

NVE

NVE is the world leader company in analog GMR sensing technology. It has a complete catalog [47] with sensors with different magnetic field range applications. Focusing on analog applications, their devices are unipolar (not able to detect sign, see Fig. 11a) and they are based on half bridges (two opposite shielded magnetoresistors) with magnetic flux concentrators. Sensitivities range from 5 to 10 mV/V/mT, with linear ranges from ± 0.1 to $\pm$ 7 mT and an input resistance of about 5 kΩ. They have described a good number of successful applications such as general magnetometry, electric current sensing, magnetic media detection and currency detection and validation.

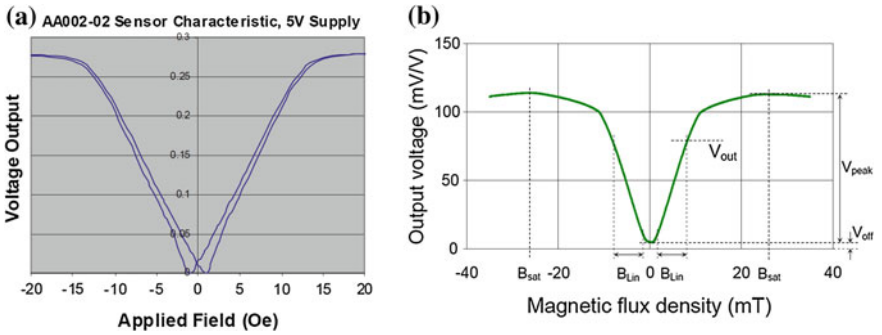

Fig. 11 Output characteristic of two representative GMR commercial sensors: **a** AA002-02 from NVE (reprinted from [47]), **b** GF705 from Sensitec (reprinted from [49])

Infineon

Infineon has developed a line of sensors mainly focusing on the automotive market, with angle sensors and encoders. They release ICs including the associated electronics. A detailed explanation of the functionality can be found in [48].

Sensitec

Sensitec has recently developed GMR sensors for general magnetic field sensing and magnetic encoding also based on unipolar half bridges (see Fig. 11b). Sensitivity is in the order of 10 mV/V/mT with linear range from ±1 to ± 8 mT and input resistance about 5 kΩ.

It is also interesting to compare the noise figure of GMR sensor against those of standard AMR and Hall based, in order to highlight their detectivity level. Such a comparison is made in Fig. 12.

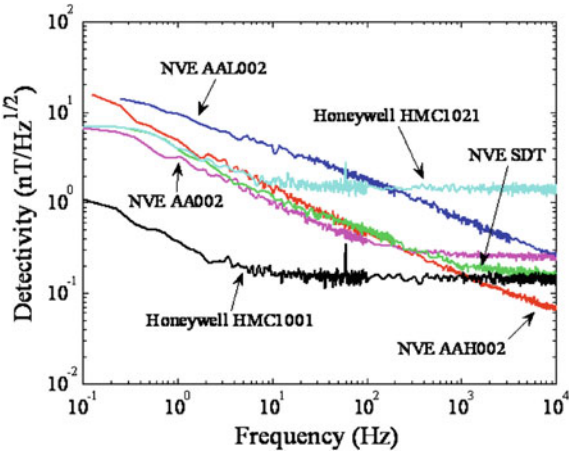

Fig. 12 Comparison of noise performance among commercially available magnetoresistive sensors (reprinted with permission from [50])

7 Successful Applications

7.1 General Magnetometry

The most of the applications developed with GMR magnetic field sensing is related to the measurement of the Earth's magnetic field perturbations produced by specifically considered ferreous body. This way, a position detecting scheme is always present.

For example, it is possible to use GMR sensors to locally measure the small magnetic perturbations caused by the iron of the car's body over the Earth's magnetic field. Moreover, if we use GMR gradient type sensors, the output signal is only dependent on the magnitude of the magnetic field variation, and no additional external magnetic field compensation is required. This way, a voltage 'signature' is obtained from the differential output of such a sensor when a car is running close to it. Within this scheme, it is easy to incorporate another sensor, placed to a well known distance in order to also measure the car speed. This proposal has been successfully developed by Pelegrí et al. [51].

The same physical principle can be directly translated to the measurement of vibrations in industrial machines. The small magnetic variations over the Earth's field produced by the vibration of the ferromagnetic pieces in industrial installations can be converted into resistance variations by the use of GMR magnetic field gradient devices. By using three sensors with the appropriated XYZ arrangement, a complete description of the vibration can be obtained. A prototype was developed by PelegrÍ et al. [52] and successfully tested with a drilling machine.

For linear magnetic position, in addition to the measurement of the Earth's field variations produced by magnetic materials, we can also use, if possible, permanent magnets associated to the moving part of the system. This way, the measurement of the absolute magnetic field is considered. Arana et al. [6] reported on the design of a high sensitivity linear position sensor using granular GMR devices. Sensitivities above 10 mV/V/mm are demonstrated by the utilization of Nd-Fe-B (0.4 T) magnets.

Angle and circular position detectors are also demanded by the industry: automotive applications, rotational machinery, etc. This kind of sensors are usually designed as contact-less systems in which a magnetic sensor (GMR in our case) detects the relative angular position of a rotationally moving magnet. This is the case presented in [53, 54]. In the first case the authors focus on their specifically designed sensor, based on a granular MR. Because of the independence on the magnetic field direction, this technology is optimal for cylindrical symmetry problems. When a NdFeB is used, sensitivities about 0.25 mV/V/° are achieved.

The conservative aerospace sector traditionally used old and well experimented components in its developments. The utilization of brand new technologies in commercial of the shelf (COTS) for space missions is nowadays only in the nearly stage. COTS are cheaper, faster in delivering and with wider reliability. Michelena et al. [55–57] introduce the possibility of using GMR commercial sensors in space

applications. GMR sensors have not been flown yet but INTA, the Spanish National Institute of Aerospace Technology is working on the adaptation of a miniaturized GMR three axis sensor (HMC2003, from Honeywell) to the attitude control system in the frame of the OPTOS project, which is a $10 \times 10 \times 10\,\text{cm}^3$ Picosat devoted to be technological test bed. The circuitry consist of conditioning and biasing electronics blocks.

7.2 Current Sensing

Electrical current can be indirectly monitored with the measurement of the generated magnetic field by means of GMR sensors. In this way, we can achieve a measurement that is sensitive, isolated and from dc up to the bandwidth of the sensors, theoretically in the range of GHz.

In the medium to high current range, a specific full bridge spin valve sensor for industrial applications is designed, characterized, implemented and tested in [58]. After soldering it onto a PCB strap, it is able to monitor currents up to 10 A. An

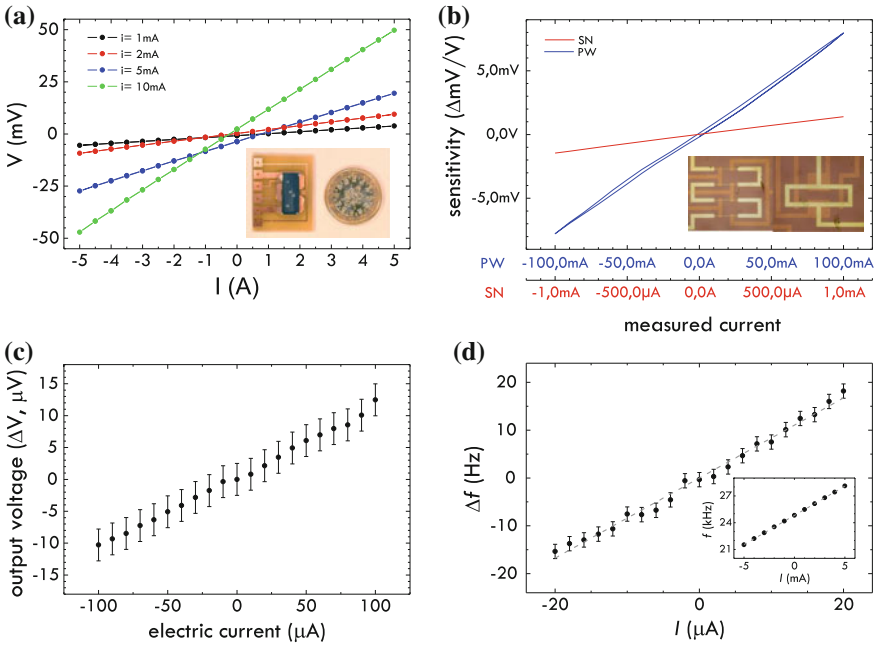

Fig. 13 Electric current sensing with GMR devices: **a** medium to high currents with an hybrid PCB-IC technology [9], **b** integrated low current measurement [22], **c** sub-mA monolithic integrated current measurement in AMS 0.35 μm chips, **d** detection improvement with the help of *V*-to-*f* schemes [31]

improved design is presented in [9] (see Fig. 13a), where a meandered strap is designed in order to give the sensor a better performance regarding voltage offset, thermal drifts and immunity against external magnetic fields. Regarding specific applications, GMR sensors have been successfully used in differential current meters [59], switching regulators [60], electrical power measurement [61] and battery management [62].

GMR based sensors have also been successfully applied to low current measurement, in different scenarios [63], in particular some compatible with CMOS technology. In this sense, we have also demonstrated the applicability of spin-valve structures [11] and bridges [22] (see Fig. 13b) to the measurement of such level electrical currents. The detectivity of such sensors can be improved by including *R*-to-*t* *V*-to-*f* schemes in the measuring process [31] (see Fig. 13c). In addition, electrical analog isolators were also designed with a basis of GMR structures [64]. Finally, the potentiality of these devices as milliwattmeters has been also demonstrated [65].

7.3 Biological

GMR sensors have been proposed for different bioapplications suchs as molecular recognition [66], bacteria analysis [67], microfluidic systems [68], hyperthermia treatments [69] or neural magnetic field detection [70].

With the rapid development of microfabrication techniques, together with the finding of compatible devices, the concept of Lab On a Chip has become more and more important in the last years. Portable devices have been recently developed which are capable of driving a fluid trough microchannels close to a detecting region, with additional conditioning and acquiring electronics. The usual scheme is the detection of the magnetic fringe field of a magnetically labeled biomolecule interaction with a complementary biomolecule bound to a magnetic field sensor. In this context, magnetoelectronics has emerged as a promising new platform technology for biosensor and biochip development [66].

8 Conclusions

GMR technology has demonstrated its maturity in its relatively short existence. It gained its popularity in the hard disks market and its success has open new doors. At this moment, only three companies develop general purpose GMR based magnetometers. But specific GMR sensors are nowadays successfully designed for *ad hoc* applications in the fields of the bio-technology, microelectronics or automotive, among others. Their intrinsic properties regarding high sensitivity, small size and compatibility with CMOS electronics allow us to be optimistic on the next future.

Acknowledgments At the personal level, we should give thanks to E. Figueras, J. Madrenas and A. Yúfera for their kindness regarding standard IC's. Also thanks to A. Roldán and J. B. Roldán for their help in developing electrical models. The authors are permanently grateful for the very fruitful collaborations with the INESC-MN. Part of the work has been carried out under projects: HP2003/0123 (*Ministry of Science and Technology, Spain*), GV05/150 (*Valencian Regional Government*), ENE2008-06588-C04-04 (*Ministry of Science and Innovation, Spain and European Regional Development Fund*), UV-INV-AE11-40892 (*Universitat de València*) and NGG-229 (2010).

References

1. M.N. Baibich, J.M. Broto, A. Fert, F.N. Vandau, F. Petroff, P. Eitenne, G. Creuzet, A. Friederich, J. Chazelas, Giant magnetoresistance of (001)Fe/(001)Cr magnetic superlattices. Phys. Rev. Lett. **61**(21), 2472–2475 (1988)
2. G. Binasch, P. Grunberg, F. Saurenbach, W. Zinn, Enhanced magnetoresistance in layered magnetic-structures with antiferromagnetic interlayer exchange. Phys Rev B **39**(7), 4828–4830 (1989)
3. S.M. Thompson, The discovery, development and future of gmr: the nobel prize 2007. J. Phys. D Appl. Phys. **41**(9), 093001 (2008)
4. U. Hartman. (Ed.), *Magnetic Multilayers and Giant Magnetoresistance: Fundamentals and Industrial Applications*. Surface Sciences (Springer, Berlin, 1999)
5. E Hirota, H Sakakima, K Inomata, *Giant Magnetoresistance Devices*. *Surface Sciences* (Springer, Berlin, 2002)
6. S. Arana, N. Arana, R. Gracia, E. Castaño, High sensitivity linear position sensor developed using granular Ag-Co giant magnetoresistances. *Sens. Actuators A—Phys* 116–121 (2005)
7. C. Reig, M. Cardoso, S.E. Mukhopadhyay, *Giant Magnetoresistance (GMR) Sensors. From Basis to State-of-the-Art Applications*. Smart Sensors, Measurement and Instrumentation (Springer, Berlin, 2013)
8. P.P. Freitas, R. Ferreira, S. Cardoso, F. Cardoso, Magnetoresistive sensors. J. Phys-Condens Matter **19**(16) 21 (2007)
9. C. Reig, D. Ramírez, F. Silva, J. Bernardo, P. Freitas, Design, fabrication, and analysis of a spin-valve based current sensor. Sens Actuators A-Phys **115**(2–3), 259–266 (2004)
10. A. Veloso, P.P. Freitas, P. Wei, N.P. Barradas, J.C. Soares, B. Almeida, J.B. Sousa, Magnetoresistance enhancement in specular, bottom-pinned, $Mn_{83}Ir_{17}$ spin valves with nano-oxide layers. Appl. Phys. Lett. **77**(7), 1020–1022 (2000)
11. C. Reig, D. Ramírez, H.H. Li, P.P. Freitas, Low-current sensing with specular spin valve structures. IEE Proc-Circ Devices Syst **152**(4), 307–311 (2005)
12. V. Peña, Z. Sefrioui, D. Arias, C. Leon, J. Santamaria, J.L. Martinez, S.G.E. te Velthuis, A. Hoffmann, Giant magnetoresistance in ferromagnet/superconductor superlattices. Phys Rev Lett **94**(5) (2005)
13. D. Pullini, D. Busquets, A. Ruotolo, G. Innocenti, V. Amigó, Insights into pulsed electrodeposition of gmr multilayered nanowires. J. Magn. Magn. Mater. **316**(2), E242–E245 (2007)
14. D. Leitao, R. Macedo, A. Silva, D. Hoang, D. MacLaren, S. McVitie, S. Cardoso, P. Freitas, Optimization of exposure parameters for lift-off process of sub-100 features using a negative tone electron beam resist, in *Nanotechnology (IEEE-NANO), 2012 12th IEEE Conference on* (2012), pp. 1–6
15. D.C. Leitao, J.P. Amaral, S. Cardoso, C. Reig, *Giant magnetoresistance (GMR) sensors. From basis to state-of-the-art applications, ch. Microfabrication techniques*. Smart Sensors, Measurement and Instrumentation [7] (2013), pp. 31–46

16. Z. Marinho, S. Cardoso, R. Chaves, R. Ferreira, L.V. Melo, P.P. Freitas, Three dimensional magnetic flux concentrators with improved efficiency for magnetoresistive sensors, J. Appl. Phys. **109**(7) (2011)
17. R.C. Jaeger, *Introduction to microelectronic fabrication*. Modular series on solid state devices (Addison-Wesley, USA, 1988)
18. J. Johnson, Thermal agitation of electricity in conductors. Nature **119**, 50–51 (Jan–Jun 1927)
19. H. Nyquist, Thermal agitation of electric charge in conductors. Phys Rev, **32**, 110–113 (Jul 1928)
20. F.N. Hooge, 1/f noise. Physica B & C **83**(1), 14–23 (1976)
21. C. Fermon, M. Pannetier-Lecoeur, *Giant magnetoresistance (GMR) sensors. From basis to state-of-the-art applications, ch. Noise in GMR and TMR sensors*. In Smart Sensors, Measurement and Instrumentation [7] (2013)
22. M. Cubells-Beltrán, C. Reig, D. Ramírez, S. Cardoso, P. Freitas, Full Wheatstone bridge spin-valve based sensors for IC currents monitoring. IEEE Sens. J. **9**(12), 1756–1762 (2009)
23. P.P. Freitas, S. Cardoso, R. Ferreira, V.C. Martins, A. Guedes, F.A. Cardoso, J. Loureiro, R. Macedo, R.C. Chaves, J. Amaral, Optimization and integration of magnetoresistive sensors. Spin **01**(01), 71–91 (2011)
24. J. Gakkestad, P. Ohlckers, L. Halbo, Compensation of sensitivity shift in piezoresistive pressure sensors using linear voltage excitation. Sens. Actuators A-Phys **49**(1–2), 11–15 (1995)
25. D.R. Muñoz, J.S. Moreno, S.C. Berga, E.C. Montero, C.R. Escrivà, A.E.N. Anton, Temperature compensation of Wheatstone bridge magnetoresistive sensors based on generalized impedance converter with input reference current. Rev. Sci. Instrum. **77**(10), 6 (2006)
26. P. Freitas, F. Silva, N. Oliveira, L. Melo, L. Costa, N. Almeida, Spin valve sensors. Sens. Actuators, A **81**(1–3), 2–8 (2000)
27. A. De Marcellis, G. Ferri, A. D'Amico, C. Di Natale, E. Martinelli, A fully-analog lock-in amplifier with automatic phase alignment for accurate measurements of ppb gas concentrations. Sens. J. IEEE **12**, 1377–1383 (2012)
28. G.T. Ong, P.K. Chan, A power-aware chopper-stabilized instrumentation amplifier for resistive wheatstone bridge sensors. Instrum. Measure. IEEE Transac. **63**, 2253–2263 (2014)
29. C. Reig, M. Cubells-Beltrán, D. Ramírez, *Giant Magnetoresistance: New Research*, *GMR Based Electrical Current Sensors* (Nova Science Publishers, New York, 2009)
30. M. Vopalensky, P. Ripka, J. Kubik, M. Tondra, Improved GMR sensor biasing design. Sens. Actuators A-Phys. **110**(1–3), 254–258 (2004)
31. A. De Marcellis, M.-D. Cubells-Beltrán, C. Reig, J. Madrenas, B. Zadov, E. Paperno, S. Cardoso, P. Freitas, Quasi-digital front-ends for current measurement in integrated circuits with giant magnetoresistance technology. Circ. Devices Syst., IET, **8**, 291–300 (July 2014)
32. W.S. Singh, B.P.C. Rao, S. Thirunavukkarasu, T. Jayakumar, Flexible GMR sensor array for magnetic flux leakage testing of steel track ropes. *J. Sens.* (2012)
33. O. Postolache, A.L. Ribeiro, H. Geirinhas Ramos, GMR array uniform eddy current probe for defect detection in conductive specimens, *Measurement* **46**, 4369–4378 (Dec 2013)
34. D.A. Hall, R.S. Gaster, T. Lin, S.J. Osterfeld, S. Han, B. Murmann, S.X. Wang, GMR biosensor arrays: a system perspective. Biosens Bioelectron. **25**, 2051–2057 (15 May 2010)
35. P. Campiglio, L. Caruso, E. Paul, A. Demonti, L. Azizi-Rogeau, L. Parkkonen, C. Fermon, M. Pannetier-Lecoeur, GMR-based sensors arrays for biomagnetic source imaging applications. IEEE Transac. Magnet. **48**, 3501–3504 (Nov 2012)
36. D.A. Hall, R.S. Gaster, K.A.A. Makinwa, S.X. Wang, B. Murmann, A 256 pixel magnetoresistive biosensor microarray in 0.18 μm CMOS. IEEE J. Solid-State Circ. **48**, 1290–1301 (May 2013)
37. J. Kim, J. Lee, J. Jun, M. Le, C. Cho, Integration of hall and giant magnetoresistive sensor arrays for real-time 2-D visualization of magnetic field vectors. IEEE Transac. Magnet. **48**, 3708–3711 (Nov 2012)

38. G.Y. Tian, A. Al-Qubaa, J. Wilson, Design of an electromagnetic imaging system for weapon detection based on GMR sensor arrays. Sens. Actuators A-Phys. **174**, 75–84 (Feb 2012)
39. H. Liu, Y.F. Zhang, Y.W. Liu, M.H. Jin, Measurement errors in the scanning of resistive sensor arrays. Sens. Actuators A: Phys. **163**(1), 198–204 (2010)
40. R. Saxena, N. Saini, R. Bhan, Analysis of crosstalk in networked arrays of resistive sensors. Sens. J. IEEE **11**, 920–924 (2011)
41. R. Saxena, R. Bhan, A. Aggrawal, A new discrete circuit for readout of resistive sensor arrays. Sens. Actuators, A **149**(1), 93–99 (2009)
42. J. Brown, A universal low-field magnetic field sensor using GMR resistors on a semicustom BiCMOS array, ed. by G. Cameron, M. Hassoun, A. Jerdee, C. Melvin. *Proceedings of the 39th Midwest Symposium on Circuits and Systems* (1996), pp. 123–126
43. S.-J. Han, L. Xu, H. Yu, R.J. Wilson, R.L. White, N. Pourmand, S.X. Wang, CMOS integrated DNA Microarray based on GMR sensors, in *2006 International Electron Devices Meeting*, International Electron Devices Meeting (2006), pp. 451–454
44. M.-D. Cubells-Beltrán, C. Reig, A.D. Marcellis, E. Figueras, A. Yúfera, B. Zadov, E. Paperno, S. Cardoso, P. Freitas, Monolithic integration of giant magnetoresistance (gmr) devices onto standard processed CMOS dies. Microelectron. J. **45**(6), 702–707 (2014)
45. F. Rothan, C. Condemine, B. Delaet, O. Redon, A. Giraud, A low power 16-channel fully integrated gmr-based current sensor, in *ESSCIRC (ESSCIRC), 2012 Proceedings of the* (2012), pp. 245–248
46. A. de Marcellis, C. Reig, M. Cubells, J. Madrenas, F. Cardoso, S. Cardoso, P. Freitas, Giant magnetoresistance (gmr) sensors for 0.35 μm cmos technology sub-ma current sensing. Proc. IEEE Sens. **2014**, 444–447 (2014)
47. NVE Corporation, GMR sensor catalog, (2012)
48. K. Kapser, M. Weinberger, W. Granig, P. Slama, *Giant Magnetoresistance (GMR) Sensors. From Basis to State-of-the-Art Applications*, *ch. GMR Sensors in Automotive Applications*. In Smart Sensors, Measurement and Instrumentation [7] (2013)
49. Sensitec, Gf705 magnetoresistive magnetic field sensor (2014)
50. N.A. Stutzke, S.E. Russek, D.P. Pappas, M. Tondra, Low-frequency noise measurements on commercial magnetoresistive magnetic field sensors. J. Appl. Phys. **97**(10) (2005)
51. J.P. Sebastiá, J.A. Lluch, J.R.L. Vizcano, Signal conditioning for GMR magnetic sensors applied to traffic speed monitoring. Sens. Actuators A-Phys. **137**(2), 230–235 (2007)
52. J.P. Sebastiá, J.A. Lluch, J.R.L. Vizcano, J.S. Bellon, Vibration detector based on gmr sensors. IEEE Trans. Instrum. Meas. **58**(3), 707–712 (2009)
53. S. Arana, E. Castaño, F.J. Gracia, High temperature circular position sensor based on a giant magnetoresistance nanogranular ag_xco_{1-x} alloy. IEEE Sens. J. **4**(2), 221–225 (2004)
54. A.J. López-Martn, A. Carlosena, Performance tradeoffs of three novel gmr contactless angle detectors. IEEE Sens. J. **9**(3), 191–198 (2009)
55. M.D. Michelena, R.P. del Real, H. Guerrero, Magnetic technologies for space: Cots sensors for flight applications and magnetic testing facilities for payloads. Sens. Lett. **5**(1), 207–211 (2007)
56. M.D. Michelena, W. Oelschlagel, I. Arruego, R.P. del Real, J.A.D. Mateos, J.M. Merayo, Magnetic giant magnetoresistance commercial off the shelf for space applications. J. Appl. Phys. **103**(7), 07E912 (2008)
57. M. Diaz-Michelena, Small magnetic sensors for space applications. Sensors **9**(4), 2271–2288 (2009)
58. J.P. Sebastiá, D.R. Munoz, P.J.P. de Freitas, W.J. Ku, A novel spin-valve bridge sensor for current sensing. IEEE Trans. Instrum. Meas. **53**(3), 877–880 (2004)
59. J. Pelegrí-Sebastiá, D. Ramírez-Muñoz, Safety device uses GMR sensor. EDN **48**(15), 84–86 (2003)
60. J. Pelegrí, D. Ramírez, P.P. Freitas, Spin-valve current sensor for industrial applications. Sens. Actuators A-Phys. **105**(2), 132–136 (2003)

61. D.R. Muñoz, D.M. Pérez, J.S. Moreno, S.C. Berga, E.C. Montero, Design and experimental verification of a smart sensor to measure the energy and power consumption in a one-phase ac line. Measurement **42**(3), 412–419 (2009)
62. D. Ramírez, J. Pelegrí, GMR sensors manage batteries. Edn **44**(18), 138 (1999)
63. M. Pannetier-Lecoeur, C. Fermon, A. de Vismes, E. Kerr, L. Vieux-Rochaz, Low noise magnetoresistive sensors for current measurement and compasses. J. Magn. Magn. Mater. **316** (2), E246–E248 (2007)
64. C. Reig, M.-D. Cubells-Beltrán, D. Ramírez, S. Cardoso, P. Freitas, Electrical isolators based on tunneling magnetoresistance technology. IEEE Trans. Magn. **44**(11), 4011–4014 (2008)
65. A. Roldán, C. Reig, M.-D. Cubells-Beltrán, J. Roldán, D. Ramírez, S. Cardoso, P. Freitas, Analytical compact modeling of GMR based current sensors: Application to power measurement at the IC level. Solid-State Electron. **54**, 1606–1612 (2010)
66. D.L. Graham, H.A. Ferreira, P.P. Freitas, Magnetoresistive-based biosensors and biochips. Trends Biotechnol. **22**(9), 455–462 (2004)
67. M. Mujika, S. Arana, E. Castaño, M. Tijero, R. Vilares, J.M. Ruano-López, A. Cruz, L. Sainz, J. Berganza, Microsystem for the immunomagnetic detection of escherichia coli o157: H7. Phys. Status Solidi A **205**(6), 1478–1483 (2008)
68. H. Ferreira, D. Graham, P. Parracho, V. Soares, P.P. Freitas, Flow velocity measurement in microchannels using magnetoresistive chips. Magnet. IEEE Transac. **40**, 2652–2654 (2004)
69. S. Mukhopadhyay, K. Chomsuwan, C. Gooneratne, S. Yamada, A novel needle-type sv-gmr sensor for biomedical applications. Sens. J. IEEE **7**, 401–408 (2007)
70. J. Amaral, S. Cardoso, P. Freitas, A. Sebastiao, Toward a system to measure action potential on mice brain slices with local magnetoresistive probes. J. Appl. Phys. **109**, 07B308–07B308–3 (Apr 2011)